Current Research in Food Science 6 (2023) 100490

Contents lists available at ScienceDirect

Current Research in Food Science

journal homepage: www.sciencedirect.com/journal/current-research-in-food-science

Spinach (*Spinacia oleracea*) microgreen prevents the formation of advanced glycation end products in model systems and breads

Qian Zhou [a], Wenxin Liang [b], Jiaqian Wan [b], Mingfu Wang [a,*]

[a] Shenzhen Key Laboratory of Food Nutrition and Health, Institute for Advanced Study, Shenzhen University, Shenzhen, 518060, China
[b] School of Biological Sciences, The University of Hong Kong, Hong Kong, 999077, China

ARTICLE INFO

Handling Editor: Yeonhwa Park

Keywords:
Microgreen
Spinach (*Spinacia oleracea*)
Advanced glycation end products (AGEs)
Bread
Functional foods

ABSTRACT

The formation of advanced glycation end products (AGEs) in daily diets poses a great threat to human health, since AGEs are closely related to some chronic metabolic diseases. In this study, we investigated the antiglycative capabilities of some popular microgreens in chemical model. Our data indicated that baby spinach (*Spinacia oleracea*) had the highest antiglycative activity during 4-wks incubation, with antioxidation being the main action route. Moreover, a bread model was set up to evaluate its antiglycative potential in real food model. The results showed that the fortification of baby spinach in bread significantly inhibited AGEs formation, with acceptable taste and food quality. Further study revealed that the antiglycative components were mainly distributed in leaves, which were separated via column chromatography and tentatively identified as chlorophyll derivatives. In summary, this study highlighted the antiglycative benefits of baby spinach which can be developed into healthy functional foods.

1. Introduction

With the increasing awareness of food quality and safety, the public has raised more demands on what and how to eat in their daily life. Microgreens emerged in time, which are defined as immature greens harvested from tender seedlings of grains, vegetables, spices, herbs, and wild relatives of crop plants (Choe et al., 2018). Often referred to as vegetable confetti, microgreens are small in body size but high in nutrition, with distinctive flavor and delicate texture. Microgreens are believed to have a great potential to be developed into new functional foods for the 21st century, since that literature data has laid a foundation for the beneficial effects of microgreens in the prevention/treatment of chronic diseases such as obesity, diabetes, and coronary heart diseases (Choe et al., 2018; Ghoora et al., 2020a,b; Kyriacou et al., 2019). This is at least partly owing to their high intensity of health-promoting phytonutrients, which including polyphenols (e.g., biflorin, quercetin rhamnoside, and isovitexin glucoside), vitamins (e.g., vitamin C, vitamin E, and vitamin K_1), carotenoids (e.g., β-carotene, violaxanthin, and lutein), essential mineral elements (e.g., Fe, Se, and Mg), and some bioactive peptides. Owing to their abundant nutritional value and huge market potential, the study of microgreens has gradually become a hotspot in the area of food science and nutrition in recent years. However, current published data of microgreens have been limited to unravel/compare their nutritional contribution between microgreens and mature greens or to address their dietary intake in food preparations in order to offer guidelines for nutritionists (Ghoora et al., 2020a,b; Mir et al., 2017; Xonti et al., 2020; Zhang et al., 2021). At present, there are already some microgreens sold in the local market of Hong Kong, such as baby spinach (*Spinacia oleracea*), baby Chinese kale (*Brassica oleracea* var. alboglabra), and pea (*Pisum sativum*) shoot. The word "baby" here is to indicate that it is young plant which harvested during early stages of plant growth, with smaller and tender leaves (Mir et al., 2017; Parwada et al., 2020). Thereinto, baby spinach is very popular from the East to the West and has received a plenty of favorites in the market.

Spinach is an annual green leafy vegetable of the *Amaranthaceae* family that grows and is eaten around the world. In household foods, spinach is often cooked via simple stir-frying and sometimes served in salads and soups, while in large-scale industrial foods, spinach is often made into spinach noodles, steamed buns, and mixed meatballs. Spinach is known to be rich in dietary fiber, chlorophyll, and trace minerals (especially Zn), providing a delicious appetite and low-fat diet. Moreover, it was reported that spinach had antioxidant, anti-inflammatory, serum lipid lowering, antimicrobial, and anticarcinogenic activity, when ingested as a food or used in the form of extract and freeze-dried

* Corresponding author.
E-mail address: mfwang@szu.edu.cn (M. Wang).

https://doi.org/10.1016/j.crfs.2023.100490
Received 13 February 2023; Received in revised form 18 March 2023; Accepted 20 March 2023
Available online 22 March 2023

powder (Roberts and Moreau, 2016). For examples, the methanolic extract of spinach prevented retinal inflammation in streptozotocin-induced diabetic rats by decreasing the level of NF-κB (nuclear factor-κB), NOX 4 (NADPH oxidase 4), and iNOS (inducible nitric oxide synthase) (Bautista-Pérez et al., 2021), spinach-rich diet inhibited brain damage in post-ischemic stroke by reducing the activity of caspase 3 in the ischemic hemisphere (Wang et al., 2005). However, previous studies usually focused on evaluating the functional properties of spinach (as a combination of various phytochemicals) in cell cultures and animal models, lacking description of the specific effective compound(s). And because of that, the application of spinach has been restricted in diets, impeding its usage in functional foods and drugs. On the other hand, recent evidences have also been exemplified in revealing the chemical profile of spinach. Of note, spinach polyphenols were identified as some phenolic acids (e.g., protocatechuic acid, *p*-coumaric acid, and ferulic acid), flavonoids (e.g., spinacetin and patuletin), flavonoid glycosides (e.g., spinacetin-3-gentiobioside and patuletin-3-gentiobioside), methoxylated flavonoids (e.g., 5, 3′,4′-trihydroxy-3methoxy-6,7-methylenedioxyflavone) (Singh et al., 2019). Thus, for the future study in this field, more attentions should be paid to connect the specific functional property of spinach with its individual active compound(s).

Protein glycation in human body happened in every moment, which is especially accelerated in the elders and people with chronic metabolic diseases. These glycated proteins are generally termed as advanced glycation end products (AGEs) and the accumulation of AGEs in the body has been linked to aging process of skin and the onset/progress/propagation of diabetes and its associated complications. Over the years, a quantity of efforts has been made in searching an appropriate strategy to delay or even avoid protein glycation. Our group also contributed some work in this field (Gao et al., 2020; Sun et al., 2019; Zhou et al., 2019a, 2019b, 2019c, 2020). For instance, we found that several plant extracts were able to prevent the formation of AGEs, such as the ethanol extract of apple (*Malus pumila* Mill) flower and Hong Dou Shan (*Taxus chinensis*) leaf tea. The active components were isolated through column chromatography and identified as flavonoids, namely, phlorizin, catechin, epicatechin, gallocatechin, and epigallocatechin (Gao et al., 2020; Sun et al., 2019). Yet few studies have reported the health benefits of microgreens in the perspective of antiglycation. In the present study, we aim to address this issue by evaluating the antiglycative effects of some popular and common microgreens, which including baby spinach, baby Chinese kale, pea shoot, baby watercress (*Nasturtium officinale*), baby amaranth (*Amaranthus tricolor* L.), baby pakchoi (*Brassica rapa* subsp. *chinensis*), and leaf of baby sweet potato (*Ipomoea batatas*). Also, the antiglycative application of microgreens in bread was investigated, considering the easily formation of AGEs in starch-based foods during baking.

2. Materials and methods

2.1. Chemicals and reagents

All microgreens were purchased from Shek Tong Tsui market (Hong Kong, China). Flour, milk powder, oil, salt, sugar, and yeast were bought from the Wellcome Supermarket (Hong Kong, China). D-glucose, fructose, methylglyoxal (MGO; 40% aqueous solution), bovine serum albumin (BSA), o-phenylenediamine (OPD), hydrochloric acid, phosphate buffer saline (PBS), 2,2-diphenyl-1-picrylhydrazyl (DPPH), β-mercaptoethanol, $NaHCO_3$, and Tris were purchased from Sigma-Aldrich (St. Louis, MO, USA). HPLC grade and LC/MS grade acetonitrile (ACN) were bought from Anaqua Chemicals Supply (HK, China). Analytical grade ethanol and methanol were from BDH Chemicals (London, UK).

2.2. Preparation of microgreen extracts

Microgreens were mashed by hand using grinding disc. After that, 20 g of each mashed sample were sonicated (40 KHz, 500 W; Kunshan Ultrasonic Instruments KQ-500E, Kunshan, China) with 100 mL ethanol for 30 min at room temperature, filtered using filter paper (Whatman, St. Louis, MO, USA). The filtrate was collected and the residue was re-sonicated with another 100 mL ethanol for 30 min. This process was repeated for 3 times. Then all filtrates were combined and vacuum evaporated to dryness under 40 °C using a rotary evaporator. The dried samples were re-dissolved in methanol to get a total volume of 10 mL extract and stored at −20 °C until use.

2.3. Antiglycative evaluation of microgreen extracts in BSA models

Both glucose-BSA (Glu-BSA) and fructose-BSA (Fru-BSA) models were set up to compare the antiglycative activity of the selected microgreens. In Glu-BSA model, 5 g BSA and 14.4 g d-glucose were added into 100 mL PBS to get a final concentration of 50 mg/mL BSA and 0.8 M glucose solution. In Fru-BSA model, 5 g BSA and 45.05 g fructose were dissolved in 100 mL PBS to get a concentration of 50 mg/mL BSA and 2.5 M fructose solution. For each BSA model, 1 mL prepared solution was mixed with each 50 μL microgreen extract, while 50 μL methanol was added into 1 mL prepared solution as a control sample. 0.2 g/L NaN_3 was added into each sample to prevent microbial growth. All prepared samples were incubated at 37 °C for 4 weeks (wks) and on every wk, 200 μL solution of each sample was transferred into black 96-well plate. The fluorescent intensity of AGEs was measured by using a Victor X4 Multilabel Plate Reader (PerkinElmer, USA) with excitation at 330 nm and emission at 410 nm. The fold change of AGEs fluorescence of each microgreen extract was calculated using the equation A and the corresponded AGEs inhibition rate was calculated using equation B (Sun et al., 2019).

$$\text{A}: \textit{Relative AGEs fluorescence} = \frac{Trt\ n}{Ctl\ 0}$$

$$\text{B}: \textit{AGEs inhibition rate}\ (\%) = \left(1 - \frac{Trt\ n}{Ctl\ n}\right) \times 100$$

Trt_n: The fluorescence of a solution with microgreen extract at the n wk; Ctl_0: The original fluorescence of a corresponded control solution; Ctl_n: The fluorescence of a corresponded control solution at the n wk.

2.4. Antioxidant evaluation of microgreen extracts

DPPH was used as a free radical source to detect the antioxidant activities of microgreen extracts (Sun et al., 2019). In brief, 50 μL of each microgreen extract or 50 μL PBS (as a control) was added into 1 mL DPPH (0.2 mM) and incubated at 37 °C for 30 min. After incubation, 150 μL of the prepared solution was transferred into a 96-well plate and measured the absorbance at 515 nm (Multiskan GO, Thermo Scientific, USA). The DPPH free radical scavenging capacity was calculated by the following equation:

$$\text{DPPH scavenging activity}\ (\%) = \left(1 - \frac{Trt}{Ctl}\right) \times 100$$

Trt: $OD_{515\ nm}$ of each microgreen extract; Ctrl: $OD_{515\ nm}$ of control.

2.5. Detection of MGO-trapping ability of microgreen extracts

The method of detecting MGO-trapping capability was referred to our previous publication (Gao et al., 2020). Briefly, 0.05 mL MGO (50 mM) was mixed with or without 0.5 mL microgreens extracts, and then PBS was added to make a final volume of 1 mL. All prepared solutions were incubated at 37 °C for 24 h. After incubation, 5 μL derivation agent OPD (500 mM) was added into each sample, vortexed for 5 s, incubated at 37 °C for 2 h. After that, cold perchloric acid (70%) was added to end the reaction. The supernatants were ready for HPLC analysis after

centrifuging at 12,000×*g* for 30 min. The HPLC system was a Waters 2695 module with a 2996 photodiode array (PDA) detector and a reversed phase (RP) C18 column (Alltima, 4.6 mm × 250 mm, 5 μm particle size; Metachem Technologies Inc., USA). 0.3% acetic acid and ACN were used as mobile phase, with gradient elution from 35–55% ACN in 21 min at 1 mL/min flow rate, and the detection wavelength was set at 316 nm. The MGO inhibition rate was calculated by the following equation:

$$\text{MGO inhibition rate } (\%) = \left(1 - \frac{Trt}{Ctl}\right) \times 100$$

Trt: The amount of MGO in the solution with microgreen extract and MGO; *Ctl*: The amount of MGO in the solution with only MGO.

2.6. Antiglycative comparison between baby and mature spinach

The antiglycative ability of baby and mature spinach was compared in Glu-BSA and Fru-BSA models following the procedure mentioned in 2.3, except that only 7 days incubation was conducted. Both of the two types of spinach were bought from the local market. After that, the edible parts of baby/mature spinach were divided into leaves and stems. And their antiglycative potentials were evaluated separately following the same procedure.

2.7. Preparation of bread

All breads were made using a bread machine (Moulinex, Ecully Cedex, France) purchased from a local market. Program 2 (500 g/each) was selected for bread making in this test. The program follows this process in sequence: first kneading (5 min), rest (5 min), second kneading (20 min), first rising (15 min), third kneading (10 s), second rising (8 min and 50 s), fourth kneading (10 s), third rising (29 min and 50 s), and baking (43 min). The recipe for original bread (as a control) was adopted from literature data (Peng et al., 2010), which included flour (350 g), milk powder (10g), sugar (16 g), salt (6 g), dried yeast (4 g), canola oil (1 tablespoon), and water (190 mL). The low level of spinach fortified-bread (LSB) was added with 80 g mashed baby spinach leaves, and the high level of spinach fortified-bread (HSB) was added with 120 g mashed baby spinach leaves. After baking, the bread was cut into 2.5 cm slices with a bread knife for the following experiments.

2.8. Sensory evaluation of baby spinach-fortified bread

Ten participants (aged 20–35 years old) were invited to join in the sensory evaluation by following the method of Heymann and Lawless (2013). Briefly, the 2.5 cm bread slices of Ctl, LSB, and HSB were prepared and put on a table. Participants were asked to taste the slices one by one and wrote down their scores individually. Six attributes were set up as appearance, color, flavor, texture, taste, and overall acceptability, regarding their degree of liking (0 = dislike, 5 = acceptable, and 10 = like very much). The scores of all participants were pooled and the average of each attribute was used to draw a Radar chart by using Microsoft Excel 2019 (Microsoft Corporation, Redmond, WA, USA).

2.9. Color characteristic of baby spinach-fortified bread

The color characteristic of bread with/without baby spinach fortification was measured by a colorimeter (CR-400, Konica Minolta, Japan) (Zhang et al., 2014). The results gave an "L^*", "a^*", and "b^*" scales. The "L^*" scale measured lightness ($L^* = 100$ means perfect white and $L^* = 0$ means black), a^* represented redness (positive)/greenness (negative), and b^* indicated yellowness (positive)/blueness (negative). ΔE was calculated by the following equation to show color change:

$$\Delta E = \sqrt{(L^*_{Trt} - L^*_{Ctl})^2 + (a^*_{Trt} - a^*_{Ctl})^2 + (b^*_{Trt} - b^*_{Ctl})^2}$$

Trt: L^*, a^*, or b^* value of baby spinach-fortified bread; *Ctl*: L^*, a^*, or b^* value of control bread.

2.10. Texture analysis of baby spinach-fortified bread

The two core slices of each bread were selected for texture analysis using TA. XT plus texture analyzer, with an aluminum plunger of 36 mm diameter. Firmness was detected based on texture profile analysis (TPA). Texture analysis was performed in the mode of "measurement of bread firmness" by ATCC method 74-09 (Peng et al., 2010). The trigger type was 5.0 g at 1.7 mm/s test speed with 10 mm compression distance. Each bread slice was tested for 3 times repeatedly and calculated the average data as the results.

2.11. Antiglycative determination of baby spinach in bread

120 mL extraction buffer (0.06 g Tween-20, 1.2 g SDS, 6 g β-mercaptoethanol, and 50 mM Tris-HCl; pH 7.4) was prepared to extract AGEs from bread (Gao et al., 2020). The upper crust, bottom crust, and core of the bread were collected separately, and were then further ground into powder. 2 g of each ground bread powder was added into 4 mL extraction buffer and all samples were incubated overnight on a shaker at room temperature. After incubation, all samples were centrifuged at 1000×*g* for 5 min, and 200 μL of each supernatant was transferred into a black 96-well plate for AGEs fluorescence detection. The fluorescent intensity of AGEs was measured with excitation at 330 nm and emission at 410 nm. The inhibition rate of AGEs in bread was calculated by the following equation:

$$\text{AGEs inhibition rate } (\%) = \left(1 - \frac{Trt}{Ctl}\right) \times 100$$

Trt: The fluorescence of baby spinach-fortified bread; *Ctl*: The fluorescence of control bread.

2.12. Antioxidant detection of baby spinach in bread

1 g mixed and ground crust was added into 2 mL 30% ethanol (in DI water), vortexed for 5 s, ultrasonically extracted for 30 min, and then centrifuged (5000×*g*, 20 min). The supernatants were collected for determining the antioxidant capacity (Teng et al., 2018). 50 μL of each supernatant or 50 μL of 30% ethanol (as a control) was added into 1 mL DPPH (0.2 mM), incubated at 37 °C for 30 min, and then the absorbance was measured by following the procedure in 2.5.

2.13. Isolation and characterization of the active components in the leaves of baby spinach

Forty grams of baby spinach leaves were ground into mash, ultrasonically extracted with 200 mL ethanol (room temperature, 30 min) for three times, and filtered by filter paper. The supernatants were combined, vacuum evaporated to dryness, and then loaded onto a 100–200 mesh silica gel column (30 × 2.5 cm). The elution buffers were 2 L hexane and 2 L methanol. 5 crude fractions were collected, vacuum evaporated to dryness, and named as SG-1 to SG-5. SG-1 (0.1 g) was yellow, SG-2 (2.1 g) was green, SG-3 (1.8 g) was thick and dark green, SG-4 (0.1 g) was breen, and SG-5 (0.5 g) was brown. An aliquot of SG-1 to SG-5 was dissolved in methanol to get a final concentration of 50 mg/mL. Then 50 μL of each aliquot was added into 1 mL Fru-BSA solution and evaluated its antiglycative ability. The most antiglycative fraction was further loaded onto a Sephadex LH-20 column (40 × 2.5 cm), eluted with 1 L methanol. 15 fine fractions were collected and re-named as SL-1 to SL-15, with the volume of 10 mL/fraction. Following that, 50 μL of each SL fraction was detected with its antiglycative effect in Fru-BSA model. The most effective SL fraction was then applied in instrumental analysis by LC-TOF/MS (SCIEX X500R, AB Sciex LLC, Toronto,

Canada). For the LC part, a RP-C18 column (YMC, 150 mm × 2 mm, 5 μm particle size; YMC Co., Ltd, Kyoto, Japan) was adopted. The injection volume was 5 μL and the flow rate was 0.5 mL/min. The mobile phase was 0.1% formic acid and ACN, with 30–90% ACN in 30 min. For the TOF/MS part, information dependent acquisition (IDA) mode was applied. Positive ionization mode was performed with MS scan from 100–1000 *m/z*. Other parameters were set according to previous published data (Zhou et al., 2021). Briefly, gas 1 (nebulizer gas) was 40 psi, gas 2 (heating gas) was 40 psi, curtain gas 30 psi, spray voltage was 5500 V, turbo spray temperature was 450 °C, collision energy (CE) in MS was 10 V and in MS/MS was 40 V.

2.14. Statistical analysis

Data were expressed as mean ± SD of at least three repeats. The one-way analysis of variance (ANOVA) was used to compare means of different groups, whilst the Tukey's test was applied for multiple comparisons of all pairs. $p < 0.05$ was considered to have statistical significance. GraphPad Prism 7.0 (GraphPad Software Inc., San Jose, CA, USA) was adopted to perform data analysis and draw figures, except the Radar chart in sensory evaluation which were performed by Microsoft Excel.

3. Results and discussion

3.1. Antiglycative screening of commercial microgreens in BSA models

According to literature data, sugar-BSA (Glu-BSA and Fru-BSA) models were set up to imitate the reaction of proteins under hyperglycemic conditions (Amani and Fatima, 2020; Gutierrez et al., 2021). In human body, glucose is the major sugar source of glycation, presenting in the form of glucose at a high concentration. Given that intracellular fructose level rarely exceeds that of glucose, recent published data pointed out that fructose is more reactive than glucose in the conjugation with proteins and the formed fructose-protein complex was differ in structure from glucose-protein conjugates (Sun et al., 2019). Also, the consumption of some diets (e.g., fruits, honey, and beverages) contributes remarkably to the body level of fructose, resulting in an accelerated *in vivo* glycation process (Aragno and Mastrocola, 2017). Thus, it is necessary to understand the performance of microgreens under these two different glycemic conditions. To begin with, we monitored the AGEs fluorescent changes of samples with/without microgreen extracts addition during 4 wks period. As shown in Fig. 1A, the AGEs fluorescence rose significantly in all samples with the increase of duration. Noteworthy, previous studies always focused on a short incubation time (namely, 1 wk) in this field (Lan et al., 2020; Wu and Yen, 2005) and our 1-wk data showed that only baby spinach, baby mustard, and pea shoot significantly attenuated the AGEs intensity. However, the interesting thing is that all of the seven microgreens had significance from the 2nd wk to the 4th wk in Glu-BSA model. On the other hand, in Fru-BSA model, all of the seven microgreens inhibited the arising trend of AGEs fluorescence during the 4 wks incubation (Fig. 1B). This might be ascribed to the more reactiveness of fructose than glucose. Therefore, our results implied that 1-wk incubation of Fru-BSA model was recommended in the study of antiglycation, instead of Glu-BSA model. And longer time (e.g., 2 wk) was suggested for Glu-BSA model.

To further understand the antiglycative effects of microgreens, their AGEs inhibition rates were calculated. As illustrated in Fig. 1C, the percentage of microgreens antiglycative rate for the 1st wk in Glu-BSA model was as follows: spinach (54.41 ± 8.90) > Chinese kale (40.66 ± 3.30) > pea (21.15 ± 5.36%) > watercress (12.69 ± 4.21) > amaranth (11.05 ± 2.81) > pakchoi (−2.12 ± 8.56) > sweet potato leaves (−11.40 ± 6.71). In the 4th wk, the order of the corresponding rate was watercress (53.11 ± 9.44) > spinach (49.82 ± 1.57) > Chinese kale (46.65 ± 3.22) > sweet potato leaves (43.39 ± 7.10) > pakchoi (40.90 ± 1.06) > pea (25.67 ± 3.60%) > amaranth (20.85 ± 2.49). Differences can be found between the 1st and 4th wk among these microgreens in the Glu-BSA model. Similar results were obtained in Fru-BSA model (Fig. 1D). Collectively, from the perspective of dynamic antiglycative activity, we can divide these microgreens into two groups: fast antiglycative microgreen (spinach, Chinese kale, pea, and amaranth) and chronic antiglycative microgreen (watercress, pakchoi,

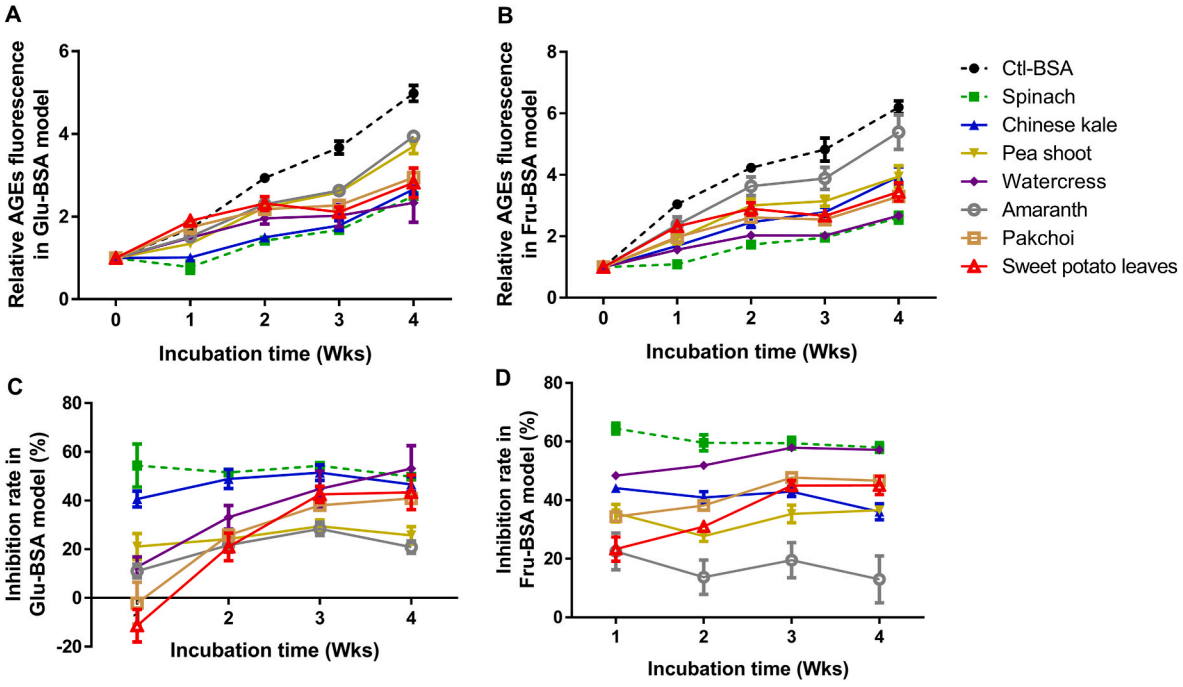

Fig. 1. Antiglycative potential of selected microgreens under long-term incubation. Relative AGEs fluorescence in Glu-BSA model (A) and Fru-BSA model (B). AGEs inhibition rate in Glu-BSA model (C) and Fru-BSA model (D). N = 5. Glu-BSA model, glucose-bovine serum albumin model; Fru-BSA model, fructose-bovine serum albumin model; AGEs, advanced glycation end products.

and sweet potato leaves). To be specific, the fast group achieved their highest AGEs inhibition rate in a shorter time (1 wk) and then remained an almost unchanged antiglycative level during 4 wks incubation. In contrast, the chronic group needed longer time (3–4 wks) to reach the peak value and their AGEs inhibition rate was raised significantly with the increasement of time. This probably owing to the structural difference of bioactive compounds in these microgreens and future attempts should be contributed to obtain a clear understanding. Moreover, baby spinach, baby Chinese kale, and baby watercress were recommended as high antiglycative vegetables suitable for daily consumption, whilst pea shoot and amaranth were low antiglycative. And baby spinach was believed to be the most antiglycative one combining the data in Fig. 1C and D, and it was chosen for further analysis in the following study.

3.2. Antioxidation as the major antiglycative pathway of baby spinach

Our previous work found that anti-oxidation and reactive dicarbonyl species (RCS)-trapping are the major antiglycative mechanisms of plant extracts (Gao et al., 2020). And this is supported by literature data (Ho et al., 2014). Hence, we evaluated the antioxidant and RCS-trapping ability of microgreens in this study. DPPH free radical scavenging capability was performed to represent their antioxidant activity and their order was as follows: sweet potato leaves (82.42 ± 0.44%) > watercress (81.41 ± 0.67%) > pakchoi (80.56 ± 1.20%) > Chinese kale(72.56 ± 2.24%)> spinach(70.56 ± 2.67%) > pea shoot (50.30 ± 2.10%) > amaranth (22.51 ± 0.53%). And based on the calculated significance, these microgreens can be categorized as high-antioxidant (sweet potato leaves, watercress, and pakchoi), medium-antioxidant (spinach and Chinese kale), and low antioxidant (pea shoot and amaranth). Intriguingly, spinach and Chinese kale had stronger antiglycative capacity, with medium antioxidant activity. Being the most important precursor of AGEs, MGO was selected as the representative RCS. The surprising thing is that the MGO-trapping capability of these microgreens was within 1–17%, with pea shoot had the highest value (16.81 ± 0.17%) and spinach had the lowest value (1.79 ± 0.59%; Fig. 2B). Combining the results in Fig. 2A and B, it can be concluded that the antiglycative potential of baby spinach should be ascribed to its antioxidant activity. In addition, as abovementioned, previous work have highlighted the importance of antioxidation and RCS-trapping in the antiglycation of natural products, especially flavonoids. For instance, the C6 and C8 positions in the A ring of apigenin are tentative to the electrophilic attack of MGO, giving rise to the generation of 6-mono MGO-apigenin adduct, 8-mono MGO-apigenin adduct, and 6, 8-di MGO-apigenin adduct (Zhou et al., 2019a). This consequently prevents AGEs formation. Considering that flavonoids are micromolecules and are simple in structure, few publications have reported similar trapping potential of macromolecules. More efforts should be contributed in this field. Also, except antioxidation and RCS-trapping, another antiglycative routes may be existed and further mechanistic studies are warranted.

3.3. Unraveling the antiglycative difference between baby and mature spinach

Literature data have exemplified that microgreens were 2–3.5 times higher in nutritional elements and bioactive compounds than mature greens cultivated under similar conditions (Ebert, 2022). And because of that, microgreens were more potential in the regulation of chronic diseases. Take baby red cabbage (purple-leaved varieties of *Brassica oleracea* Capitata Group) as an example. Baby red cabbages reduced high fat diet-induced weight gain, probably owing to their high level of retinoic acid (a metabolite of β-carotene) and idole-3-carbinal which can prevent adipogenesis (Choe et al., 2018; Ghoora et al., 2020). In the present study, our data revealed that no significant antiglycative differences can be calculated between baby and mature spinach in both BSA models (Fig. 3A and B). Also, our results showed that spinach leaves were 1.3–5.2 times higher in antiglycation than their corresponded spinach stems. And again, no significance was found between baby spinach leaves/stems and mature spinach leaves/stems in BSA models. Since that this commercial baby/mature spinach might be grown in different environment, our current data was not sufficient to conclude that baby and mature spinach had similar antiglycative capability. To address this issue, future experiments are needed to monitor the capability of spinach during growth. In general, our data implied the beneficial effects of consuming spinach leaves in the perspective of antiglycation.

3.4. Evaluation of baby spinach-fortified bread as an antiglycative food

Bread has a broad acceptance of consumers around the world, due to its favorable taste and a great possibility of variations. It is also a good source of functional foods which represents an easy and convenient screening carrier for healthy components. In the past decades, there was an increase trend in fortifying bread with fruits and vegetables to offer additional benefits for human health. For instance, blueberry (*Vaccinium*

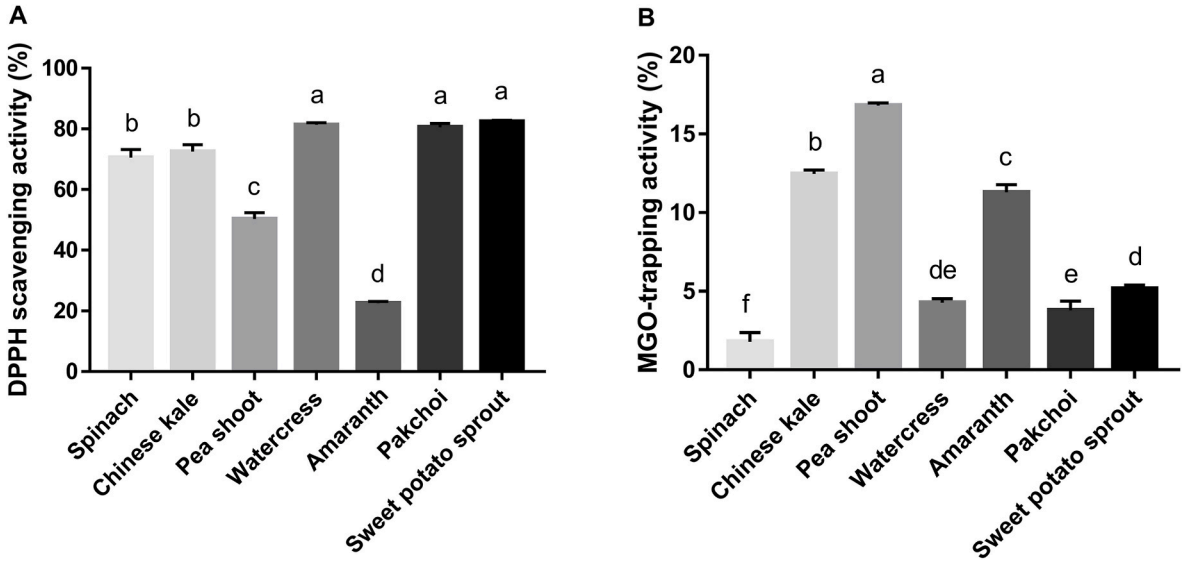

Fig. 2. Antiglycative mechanism analysis of selected microgreens. A: DPPH scavenging activity. B: MGO-trapping activity. Columns with different characters are significantly different ($p < 0.05$). N = 3. DPPH, 2,2-diphenyl-1-picrylhydrazyl; MGO, methylglyoxal.

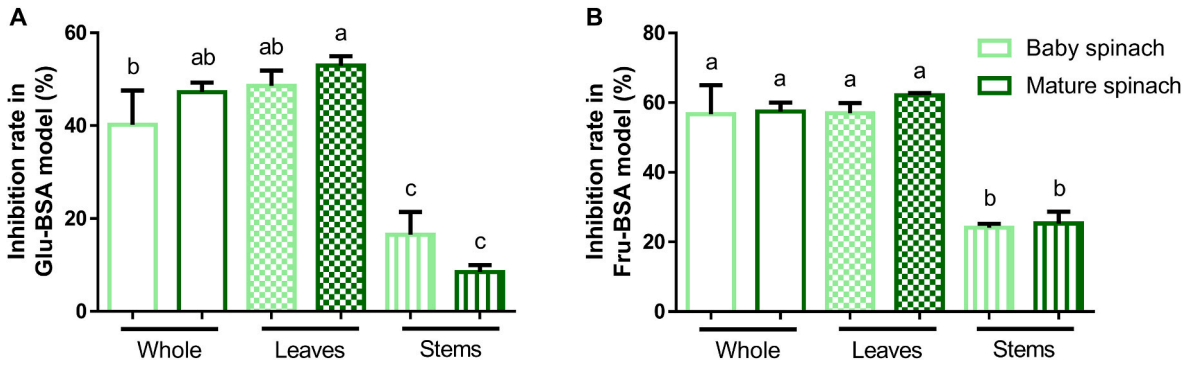

Fig. 3. The comparison of antiglycative activity between baby and mature spinach in Glu-BSA model (A) and Fru-BSA model (B). Columns with different characters are significantly different ($p < 0.05$). N = 3. Glu-BSA model, glucose-bovine serum albumin model; Fru-BSA model, fructose-bovine serum albumin model.

genus) bread was distinguished owing to their high level of anthocyanins and pumpkin (*Cucurbita* genus) bread offered a characteristic color with high carotenoids content (Betoret and Rosell, 2020). By far, no microgreens-enriched baking food has been found in the market and few literature data has contributed in this area, although microgreens were reported to possess stronger bioactivity (Wojdyło et al., 2020). In this study, two level of spinach bread, LSB (80 g spinach leaves in 350 g flour) and HSB (120 g spinach leaves in 350 g flour), were prepared on our pre-experiments. 120 g spinach leaves were the highest amount that can be added into the bread. Otherwise, the final product cannot form a regular shape using the bread-making machine. Besides, 80 g spinach leaves were the level that able to offer characteristic flavor. Fig. 4A showed the appearance of breads with/without spinach addition. A greener color and fewer irregularly shaped excavations were presented in spinach-enriched breads. Sensory evaluation was performed to acquire consumers' preference on the fortification of spinach into breads by using quantitative descriptive analysis. The participants' age was within 20–35 years old because bread consumption was more popular in

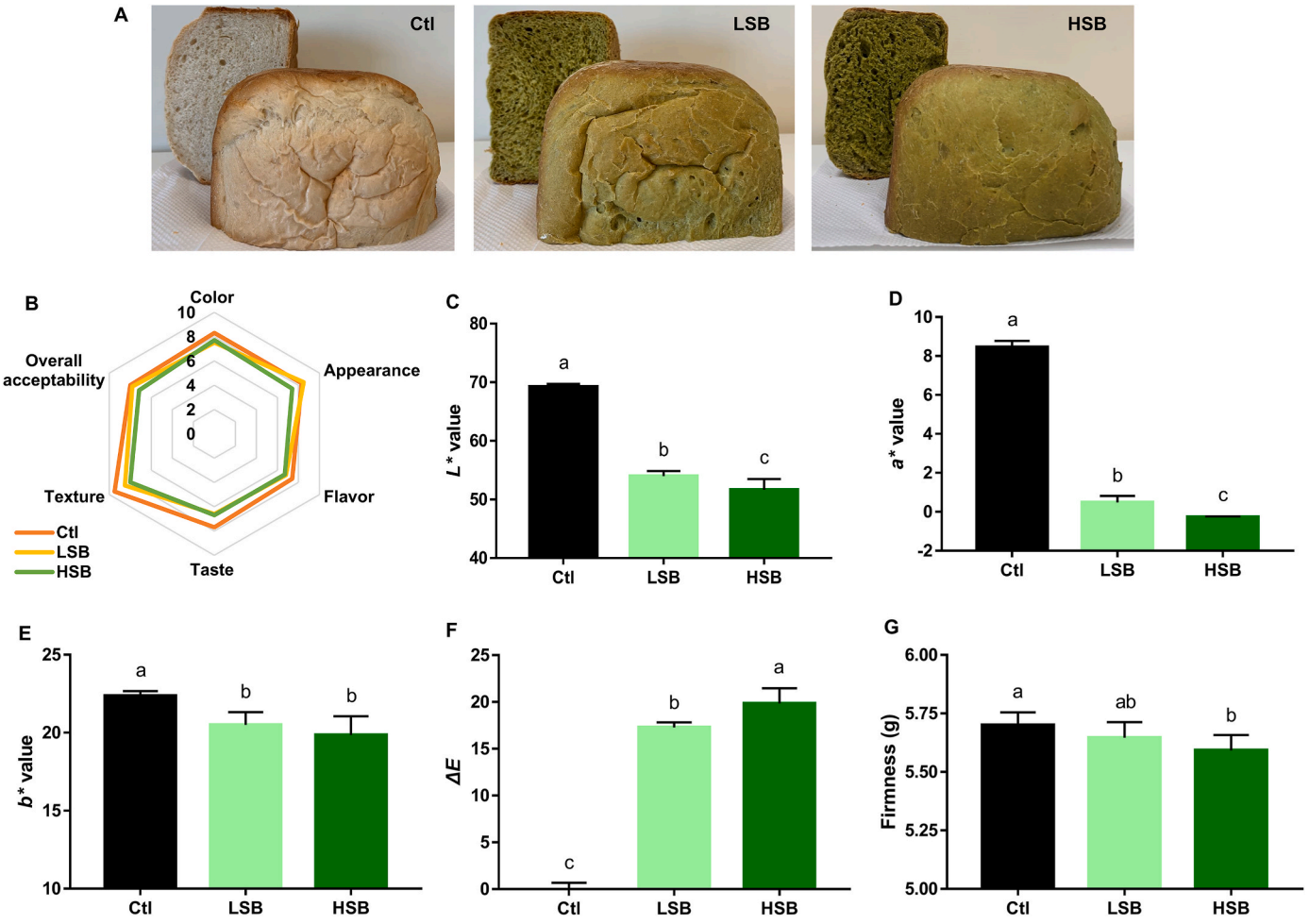

Fig. 4. Sensory evaluation and food quality measurements of baby spinach-fortified bread. A: Represented picture of bread fortified with/without baby spinach leaves. B: Radar chat of sensory evaluation (N = 10). C–E: Lab value (N = 3). F: Calculated ΔE value (N = 3). H: Firmness (N = 10). Columns with different characters are significantly different ($p < 0.05$). Ctl, control; LSB, low level of spinach fortified-bread; HSB, high level of spinach fortified-bread.

younger generation (Engindeniz and Bolatova, 2021). Compare with Ctl, LSB was mainly low in taste and texture, while HSB was low in all of the five attributes. But no significance can be calculated (Fig. 4B). Furthermore, the color (Lab value) and firmness changes of breads were chosen as representative physical measurements to characterize the food quality. As shown in Fig. 4C–F, spinach addition reduced L^* and a^* value in a dose-dependent manner, indicating darkness and greenness in spinach breads. It also decreased b^* value, but with no difference between LSB and HSB. Color distances were presented by ΔE value, which was 17.28 and 19.85 in LSB and HSB, comparing with Ctl. The firmness of breads was measured by a texture analyzer. The interesting thing is that no significance was found between Ctl and LSB, and between LSB and HSB. But HSB was significantly softer than Ctl (Fig. 4G).

Several lines of evidence supported that starch-based foods (e.g., breads) were prone to produce toxic AGEs during thermal process (Peng et al., 2011). Considering that the original volume of our bread was big, the formed AGEs in different part of bread might be differed from each other. Hence, the AGEs fluorescence of the upper crust, bottom crust, and core of the breads were detected separately in this study. As illustrated in Fig. 5A, AGEs were mainly generated in the crust, with no significance between upper and bottom crust. However, the core of the bread only contributed 23–45% of the Ctl upper crust. This indicated that heat-induced AGEs were more likely to be formed on food surface. Besides, the addition of spinach had little antiglycative influence on the bread core since that no significant difference was found between Ctl and the two spinach-fortified breads. The AGEs inhibition rate of spinach in bread crust was further calculated and the corresponded results were 29.32 ± 4.43% (upper crust) and 34.90 ± 1.76% (bottom crust) in LSB, 57.18 ± 8.17% (upper crust) and 43.11 ± 5.15% (bottom crust) in HSB, respectively (Fig. 5B). Therefore, our data confirmed that spinach can display appreciable antiglycative effect in breads. As aforementioned in part 3.2, antioxidation worked as the major antiglycative mechanism of spinach in BSA models, thus the antioxidant potential of spinach in bread was also measured. As elucidated in Fig. 5C, the DPPH free radical scavenging rates in bread crust of Ctl, LSB, and HSB were 8.46 ± 1.12, 18.85 ± 1.64, and 15.24 ± 1.64, respectively. Intriguingly, the Ctl bread itself also possessed slight antioxidant capability and this was supported by literature data (Yu et al., 2013). And spinach fortification can significantly improve the antioxidant activity of bread. Collectively, our data suggested the antiglycative benefits of baby spinach-enriched bread, which had acceptable taste and food quality.

3.5. Characterization of the antiglycative components in the leaves of baby spinach

To identify the active components in the leaves of baby spinach, an antiglycative activity-guided screening platform was set up (Fig. 6A). In brief, the ethanolic extracts of microgreens were evaluated of their AGEs inhibition rate in Fru-BSA model. The most effective one, which was baby spinach in this case, was chosen for further open column chromatographic analysis by Silica gel and Sephadex LH-20, successively. Five crude fractions were obtained from silica gel column. Their antiglycative ability was assessed, with SG-3 and SG-4 fraction having the highest inhibition rate (Fig. 6B). Only 0.1 g SG-4 was found, which was not enough for further column separation. Therefore, SG-3 was again

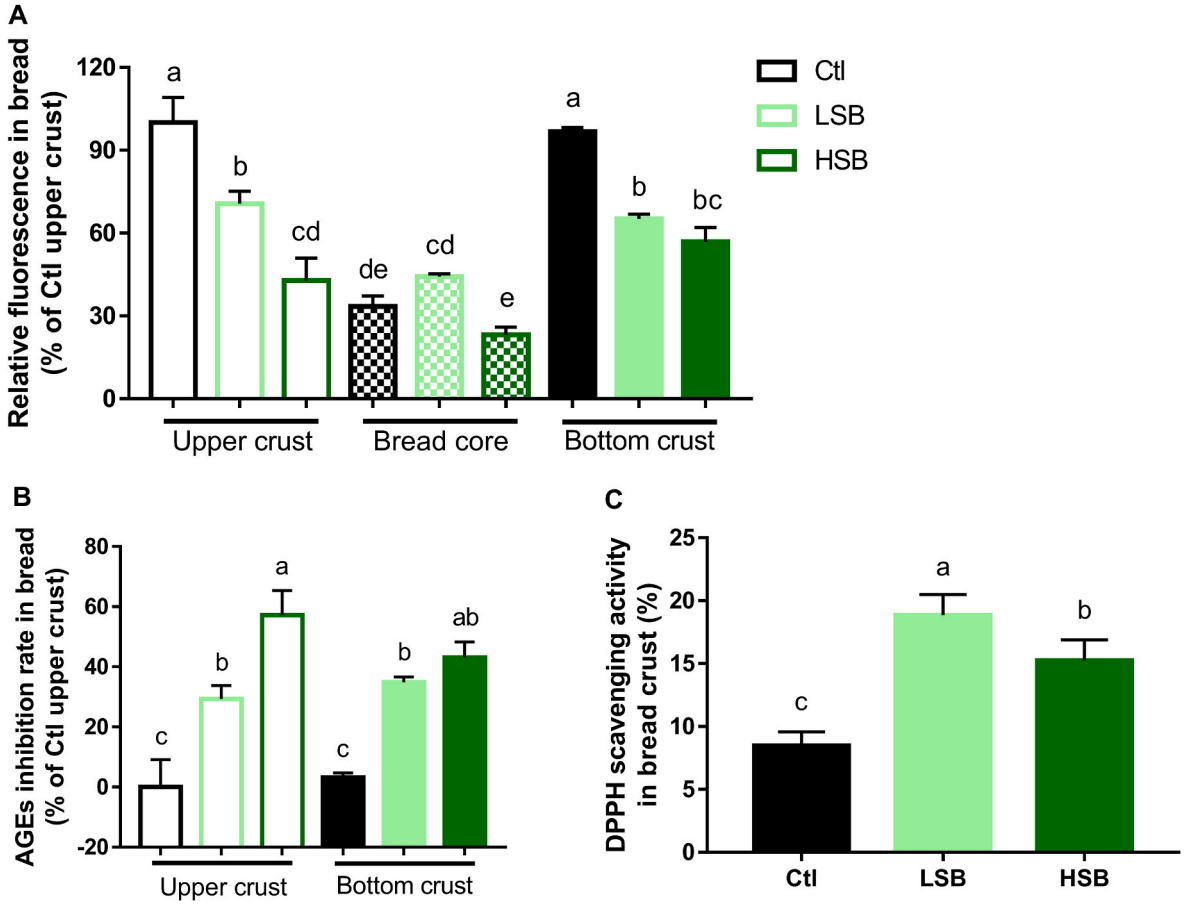

Fig. 5. Antiglycative evaluation of baby spinach in bread. A: Relative AGEs fluorescence in breads. B: AGEs inhibition rate in breads. C: DPPH scavenging rate in breads. N = 3. Ctl, control; LSB, low level of spinach fortified-bread; HSB, high level of spinach fortified-bread; AGEs, advanced glycation end products; DPPH, 2,2-diphenyl-1-picrylhydrazyl.

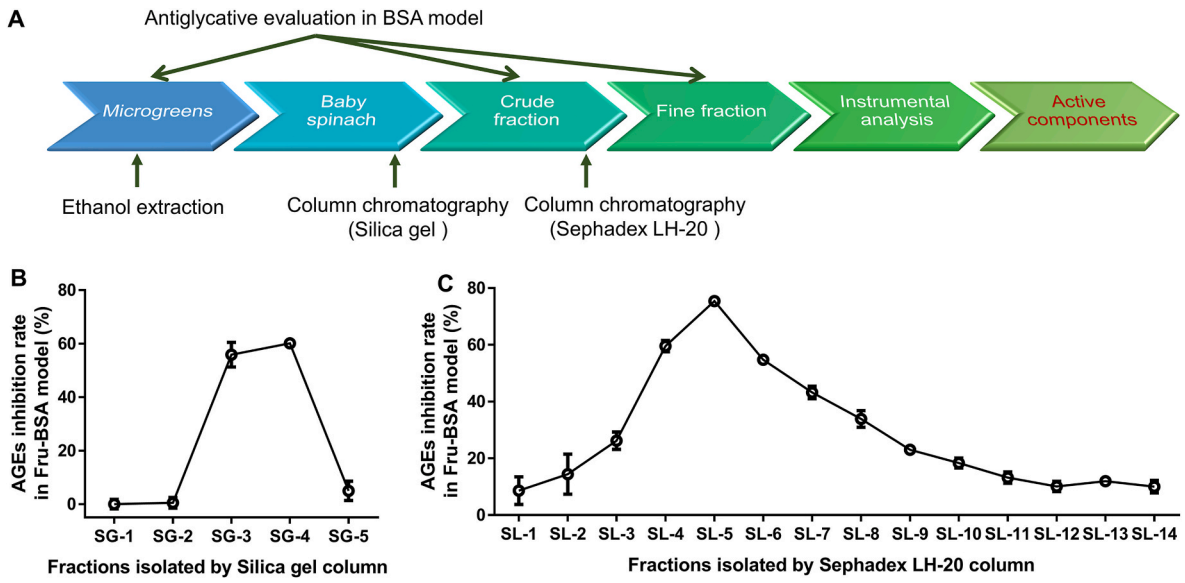

Fig. 6. Characterization of active components in baby spinach. A: Illustration of antiglycative activity guided-screening platform. B: AGEs inhibition rate of eluents from silica gel isolation. C: AGEs inhibition rate of eluents from Sephadex LH-20 isolation. N = 3. BSA, bovine serum albumin; AGEs, advanced glycation end products; SG-1~SG-5, silica gel column eluted fractions; SL-1~SL-14, Sephadex LH-20 column eluted fractions.

loaded onto Sephadex LH-20 column and then 15 fine eluents were collected. Further antiglycative analysis found SL-5 (clear green solution) had a remarkable inhibition rate at 75.44 ± 0.98% (Fig. 6C). Following that, SL-5 was subject into LC-TOF/MS analysis. By referring to Mass Bank and previous published data (Agarwal and Gupta, 2018), the compounds in SL-5 with an intensity of $\geq 1 \times 10^7$ were presented in Fig. 7A and B. More specifically, two chlorophyll derivatives were tentatively identified, namely, pheophorbide a ($[M+H]^+ = 593.2748$) and pyropheophorbide a ($[M+H]^+ = 535.2698$).

4. Conclusions

The present study assessed the potential benefits of some popular microgreens in the local market of Hong Kong from the perspective of antiglycation. Our results revealed that baby spinach, baby Chinese kale, and baby watercress can be consumed as high antiglycative vegetables suitable in daily diets, whilst pea shoot and baby amaranth were low antiglycative. Thereinto, baby spinach was the most antiglycative one and was further evaluated its potential in bread. By referring to sensory evaluation data and physio measurements, baby spinach-fortified bread

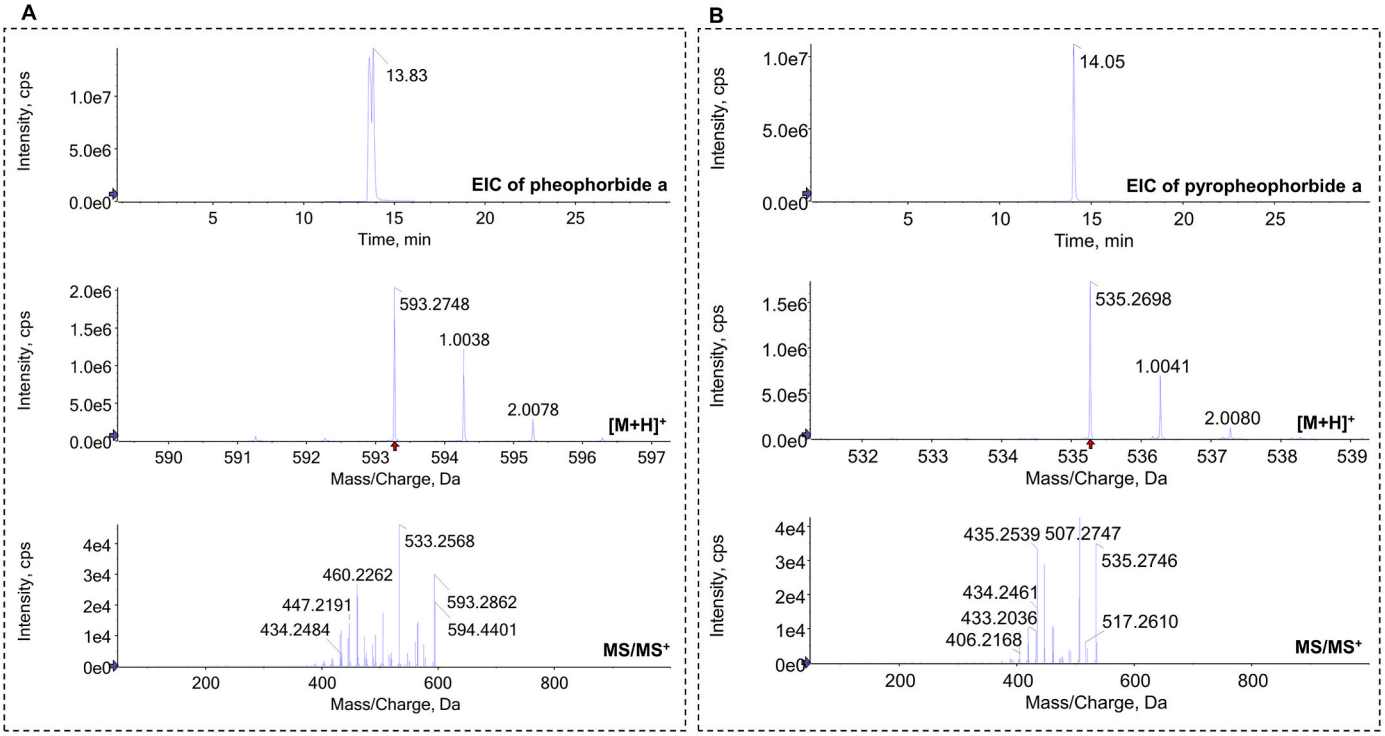

Fig. 7. MS spectra of pheophorbide a (a) and pyropheophorbide a (b) from SL-5 fraction. SL-5, the 5th eluted fraction from Sephadex LH-20 column; EIC, extracted ion chromatogram.

was regarded as acceptable in taste and food quality, which also exerted appreciable antioxidant capability in real food model. However, our data showed that baby and mature spinach had no antiglycative difference. This was differed from previous data which mentioned significantly more benefits of microgreens than mature greens. In addition, a platform for antiglycative activity-guided screening was set up by combing sugar-BSA model assessment and open column chromatographic analysis. And the active components of baby spinach were found to mainly distributed in the leaves and were tentatively identified as chlorophyll derivatives.

Source of funding

This work was partly supported by the National Natural Science Foundation of China (No. 32101935), the National Key R&D Program of China (No. 2021YFD2100103), and the Guangdong Basic and Applied Basic Research Foundation (No. 2022A1515012098).

CRediT authorship contribution statement

Qian Zhou: Methodology, Formal analysis, Investigation, Resources, Writing – original draft, Writing – review & editing, Funding acquisition. **Wenxin Liang:** Methodology, Writing – original draft. **Jiaqian Wan:** Methodology, Writing – original draft. **Mingfu Wang:** Conceptualization, Writing – review & editing, Supervision, Project administration, Funding acquisition.

Declaration of competing interest

The authors declare that they have no known competing financial interests or personal relationships that could have appeared to influence the work reported in this paper.

Data availability

Data will be made available on request.

Acknowledgments

The authors thank Ms. Dorothy M. C. Chan for her technical assistance.

References

Agarwal, A., Gupta, S.D., 2018. Assessment of spinach seedling health status and chlorophyll content by multivariate data analysis and multiple linear regression of leaf image features. Comput. Electron. Agric. 152, 281–289.
Amani, S., Fatima, S., 2020. Glycation with fructose: the bitter side of nature's own sweetener. Curr. Diabetes Rev. 16 (9), 962–970.
Aragno, M., Mastrocola, R., 2017. Dietary sugars and endogenous formation of advanced glycation endproducts: emerging mechanisms of disease. Nutrients 9 (4), 385.
Bautista-Pérez, R., Cano-Martínez, A., Gutiérrez-Velázquez, E., Martínez-Rosas, M., Pérez-Gutiérrez, R.M., Jiménez-Gómez, F., Flores-Estrada, J., 2021. Spinach methanolic extract attenuates the retinal degeneration in diabetic rats. Antioxidants 10 (5), 717.
Betoret, E., Rosell, C.M., 2020. Enrichment of bread with fruits and vegetables: trends and strategies to increase functionality. Cereal Chem. 97 (1), 9–19.
Choe, U., Yu, L.L., Wang, T.T., 2018. The science behind microgreens as an exciting new food for the 21st century. J. Agric. Food Chem. 66 (44), 11519–11530.
Ebert, A.W., 2022. Sprouts and microgreens—novel food sources for healthy diets. Plants 11 (4), 571.
Engindeniz, S., Bolatova, Z., 2021. A study on consumption of composite flour and bread in global perspective. Br. Food J. 123 (5), 1962–1973.
Gao, J., Sun, Y., Li, L., Zhou, Q., Wang, M., 2020. The antiglycative effect of apple flowers in fructose/glucose-BSA models and cookies. Food Chem. 330, 127170.
Ghoora, M.D., Babu, D.R., Srividya, N., 2020a. Nutrient composition, oxalate content and nutritional ranking of ten culinary microgreens. J. Food Compos. Anal. 91, 103495.
Ghoora, M.D., Haldipur, A.C., Srividya, N., 2020b. Comparative evaluation of phytochemical content, antioxidant capacities and overall antioxidant potential of select culinary microgreens. Journal of Agriculture and Food Research 2, 100046.
Gutierrez, J.A., Liu, W., Perez, S., Xing, G., Sonnenberg, G., Kou, K., Vera, N.B., 2021. Pharmacologic inhibition of ketohexokinase prevents fructose-induced metabolic dysfunction. Mol. Metabol. 48, 101196.
Heymann, H., Lawless, H.T., 2013. Sensory Evaluation of Food: Principles and Practices. Springer Science and Business Media, New York.
Ho, S.C., Chang, P.W., Tong, H.T., Yu, P.Y., 2014. Inhibition of fluorescent advanced glycation end-products and N-carboxymethyllysine formation by several floral herbal infusions. Int. J. Food Prop. 17 (3), 617–628.
Kyriacou, M.C., El-Nakhel, C., Graziani, G., Pannico, A., Soteriou, G.A., Giordano, M., Rouphael, Y., 2019. Functional quality in novel food sources: genotypic variation in the nutritive and phytochemical composition of thirteen microgreens species. Food Chem. 277, 107–118.
Lan, M.Y., Li, H.M., Tao, G., Lin, J., Lu, M.W., Yan, R.A., Huang, J.q., 2020. Effects of four bamboo derived flavonoids on advanced glycation end products formation in vitro. J. Funct.Foods 71, 103976.
Mir, S.A., Shah, M.A., Mir, M.M., 2017. Microgreens: production, shelf life, and bioactive components. Crit. Rev. Food Sci. Nutr. 57 (12), 2730–2736.
Parwada, C., Chigiya, V., Ngezimana, W., Chipomho, J., 2020. Growth and performance of baby spinach (Spinacia oleracea L.) grown under different organic fertilizers. International Journal of Agronomy 1–6, 2020.
Peng, X., Ma, J., Chen, F., Wang, M., 2011. Naturally occurring inhibitors against the formation of advanced glycation end-products. Food Funct. 2 (6), 289–301.
Peng, X., Ma, J., Cheng, K.W., Jiang, Y., Chen, F., Wang, M., 2010. The effects of grape seed extract fortification on the antioxidant activity and quality attributes of bread. Food Chem. 119 (1), 49–53.
Roberts, J.L., Moreau, R., 2016. Functional properties of spinach (Spinacia oleracea L.) phytochemicals and bioactives. Food Funct. 7 (8), 3337–3353.
Singh, A., Singh, P., Kumar, B., Kumar, S., Dev, K., Maurya, R., 2019. Detection of flavonoids from Spinacia oleracea leaves using HPLC-ESI-QTOF-MS/MS and UPLC-QqQLIT-MS/MS techniques. Nat. Prod. Res. 33 (15), 2253–2256.
Sun, M., Shen, Z., Zhou, Q., Wang, M., 2019. Identification of the antiglycative components of Hong Dou Shan (Taxus chinensis) leaf tea. Food Chem. 297, 124942.
Teng, J., Liu, X., Hu, X., Zhao, Y., Tao, N.P., Wang, M., 2018. Dihydromyricetin as a functional additive to enhance antioxidant capacity and inhibit the formation of thermally induced food toxicants in a cookie model. Molecules 23 (9), 2184.
Wang, Y., Chang, C.F., Chou, J., Chen, H.L., Deng, X., Harvey, B.K., Bickford, P.C., 2005. Dietary supplementation with blueberries, spinach, or spirulina reduces ischemic brain damage. Exp. Neurol. 193 (1), 75–84.
Wojdyło, A., Nowicka, P., Tkacz, K., Turkiewicz, I.P., 2020. Sprouts vs. microgreens as novel functional foods: variation of nutritional and phytochemical profiles and their in vitro bioactive properties. Molecules 25 (20), 4648.
Wu, C.H., Yen, G.C., 2005. Inhibitory effect of naturally occurring flavonoids on the formation of advanced glycation endproducts. J. Agric. Food Chem. 53 (8), 3167–3173.
Xonti, A., Hunter, E., Kulu, N., Maboeei, P., Stander, M., Kossmann, J., Loedolff, B., 2020. Diversification of health-promoting phytochemicals in radish (Raphanus raphanistrum) and kale (Brassica oleracea) micro-greens using high light bio-fortification. Functional Foods in Health and Disease 10 (2), 65–81.
Yu, L., Nanguet, A.L., Beta, T., 2013. Comparison of antioxidant properties of refined and whole wheat flour and bread. Antioxidants 2 (4), 370–383.
Zhang, X., Chen, F., Wang, M., 2014. Antioxidant and antiglycation activity of selected dietary polyphenols in a cookie model. J. Agric. Food Chem. 62 (7), 1643–1648.
Zhang, Y., Xiao, Z., Ager, E., Kong, L., Tan, L., 2021. Nutritional quality and health benefits of microgreens, a crop of modern agriculture. Journal of Future Foods 1 (1), 58–66.
Zhou, Q., Cheng, K.W., Gong, J., Li, E.T., Wang, M., 2019a. Apigenin and its methylglyoxal-adduct inhibit advanced glycation end products-induced oxidative stress and inflammation in endothelial cells. Biochem. Pharmacol. 166, 231–241.
Zhou, Q., Cheng, K.W., Xiao, J., Wang, M., 2020. The multifunctional roles of flavonoids against the formation of advanced glycation end products (AGEs) and AGEs-induced harmful effects. Trends Food Sci. Technol. 103, 333–347.
Zhou, Q., Gong, J., Wang, M., 2019b. Phloretin and its methylglyoxal adduct: implications against advanced glycation end products-induced inflammation in endothelial cells. Food Chem. Toxicol. 129, 291–300.
Zhou, Q., Wang, L., Liu, B., Xiao, J., Cheng, K.W., Chen, F., Wang, M., 2021. Tricoumaroylspermidine from rose exhibits inhibitory activity against ethanol-induced apoptosis in HepG2 cells. Food Funct. 12 (13), 5892–5902.
Zhou, Q., Xu, H., Yu, W., Li, E., Wang, M., 2019c. Anti-inflammatory effect of an apigenin-maillard reaction product in macrophages and macrophage-endothelial cocultures. Oxid. Med. Cell. Longev., 9026456, 2019.